AIAA 2013-5178

Evaluation of Aircraft Contrails using Dynamic Dispersion Model

Jinhua Li*
Stinger Ghaffarian Technologies, Moffett Field, CA

Fabio Caiazzo †, Steven Barrett ‡
Massachusetts Institute of Technology, Cambridge, MA

Neil Chen §, Banavar Sridhar ¶
NASA Ames Research Center, Moffett Field, CA

Hok K. Ng ‖
University of California, Santa Cruz, CA

In this paper, an aircraft contrail model developed by researchers at NASA Ames Research Center assuming static atmospheric conditions is extended to simulate the dynamic evolution of contrails triggered by airborne flights. A Lagrangian dispersion model and a cloud microphysics model were added to create the new dynamic contrail model to simulate the physical processes of contrail ice particle formation, growth, advection, and dissipation. The dynamic contrail model can simulate the full life cycle of young-age linear contrails in any day for the entire continental U.S. airspace with real-time meteorological and air traffic data in less than 6 hours. The aircraft-induced contrails weighted by their ages are also calculated to assess the impact at different air traffic control centers.

I. Introduction

Young-age contrails are long, thin, and linear artificial clouds that are sometimes visible from the ground. They are formed behind aircraft cruising near the tropopause because of mixing of water vapor emitted from jet engines with cold and ice-saturated ambient air. Persistent contrails can last many hours to a day before dissipation or turning into cirrus cloud in favorable meteorological conditions. They consist of ice crystals condensed on aerosols. Linear contrails also grow by uptake of ambient water and grow in size by diffusive spread over a large airspace. Recent studies have shown that aircraft-induced persistent contrails may have negative long-term impacts on the global climate by reflecting solar short-wave radiation and trapping outgoing long-wave radiation.[1–3] An estimation of average aviation-induced linear contrail and contrail cirrus cloud radiative forcing is in the range of $13 - 87 mW/m^2$, exceeding that of aircraft CO_2 emissions.[4]

A number of computational models have been developed to simulate aircraft contrails in recent years.[5–11] Those models are capable of simulating the partial or full life cycle of the aircraft contrails, which starts from a few seconds after initial ice particle formation, extends to young-age linear contrails advection (or transport) after a few hours, and finally ends with dissipation or transformation into cirrus clouds up to one day. Researchers at Stanford University developed a low-order contrail model and a Large Eddy Simulation (LES) model.[6,9,10] The LES can model the first one or two minutes of contrail ice crystal formation immediately following aircraft engines and movement driven by aircraft wingtip vortices and engine exhausts. The outputs from LES including ice crystal sizes were then fed into a set of low-order difference equations as the initial conditions to compute the linear contrail trajectories driven by the wind, assuming Lagrangian dispersion model. Burkhardt and Kärcher at German Aerospace Center (DLR)[5] developed a contrail cirrus cloud

*Research Scientist, AIAA member
†Graduate Student, Department of Aeronautics and Astronautics
‡Assistant Professor, Department of Aeronautics and Astronautics
§Research Aerospace Engineer, Aviation Systems Division, AIAA member
¶Senior Scientist for Air Transportation Systems, AIAA fellow
‖Senior Software Engineer, AIAA member

model based on physical processes. The contrail cirrus cloud is represented by its fractional coverage, length, and ice-water mass mixing ratio. The dynamic processes of the contrail cirrus cloud model include contrail formation, transport, spread, deposition, sublimation, and precipitation. More recently, a comprehensive contrail cirrus computational model and simulation software, called Contrail Cirrus Prediction Tool (CoCiP), has been developed at DLR.[11] The software simulates the full aircraft contrail life cycle and computes the associated climate impact.

Researchers at NASA Ames Research Center have developed a simplified aircraft contrail model, which simulates the aircraft-induced contrail formation only based on the Appleman criterion and using static atmospheric conditions.[7,8] However, based on both theory of cloud microphysics and evidence from satellite images,[12,13] aircraft contrails are a dynamic process, like natural cirrus cloud, which normally lasts a few hours. In this paper, that model is extended to include the dynamic transport of contrails by adding a Lagrangian dispersion model and a cloud microphysics model. The newly-added computational methods are based on well-established results in related fields.[14–16] To the best of our knowledge, the proposed dynamic contrail model is based on the same basic cloud physics, but computationally more efficient compared with Stanford's and DLR's aircraft contrail models, mainly because of the following assumptions: (1) It does not include the initial contrail ice particles down-wash process by airplane wake vortex turbulence. The physical process normally takes less than one or two minutes. It determines the initial contrail ice particle sizes and displacements. Based on our knowledge, wake vortex turbulence simulation is very time-consuming. To save computation time, the average initial ice particle size is used. The initial contrail location is assumed to be at the cell, where the contrail formation conditions are satisfied; (2) The clouds are assumed to have uniform ice particle (or ice water content) density. Wind tilting effect is not considered; (3) The proposed dynamic contrail model does not consider the interaction between contrail clouds and natural cirrus clouds; and (4) The results do not include the additional radiative forcing caused by aircraft contrails, which measures the global temperature change. We are working towards adding a contrail radiative forcing computation module that can compute the total aircraft contrails radiative forcing using the inputs from the current model such as ice particle size and contrail cloud horizontal cover area.

Although the progress has been made in aviation-induced contrails simulation from above, it remains a challenging task to validate the simulated contrail tracks, cloud coverages and global radiative forcing resulting from those contrails. It is mainly because of the large temporal scale of contrail life cyle and spatial scale of contrail extension, limited knowledge and uncertainties on some complex physical processes and lack of direct observation data from satellites as discussed in reference[17].

Figure 1 summarizes the dynamic contrail model structure with changes from previous work within the dashed rectangle.[7,8] The results can be used to measure the long-term climate impact of the aviation-induced linear contrails and design the aircraft operation strategies to reduce the contrail environmental impact (e.g. references[18,19]).

The rest of the paper is organized as follows: Section II presents the model mathematical equations. In Section III, the proposed model is applied with U.S. air traffic and meteorological data from a single day. New metrics are proposed to measure the aircraft contrails predicted by the dynamic model. Finally, Section IV is the conclusion.

II. Dynamic Aircraft Contrail Model

II.A. Persistent contrail formation condition and persisting condition

The atmospheric conditions required for aircraft contrail formation are well understood. They are based on atmospheric thermodynamics and specified by the Appleman criterion.[20,21] Persistent linear contrails are formed shortly after aircraft fly through a region of airspace, in which the relative humidity and temperature of the ambient air satisfy all the following equations:[22]

$$\begin{cases} RH_i > 100\%, \\ RH_w > r_{contr}, \\ RH_w < 100\%, \text{ and} \\ T < T_{contr}, \end{cases} \tag{1}$$

where RH_w is the relative humidity with respect to water and T is the temperature. Both can be directly extracted from meteorological data such as National Oceanic and Atmospheric Administration (NOAA)'s

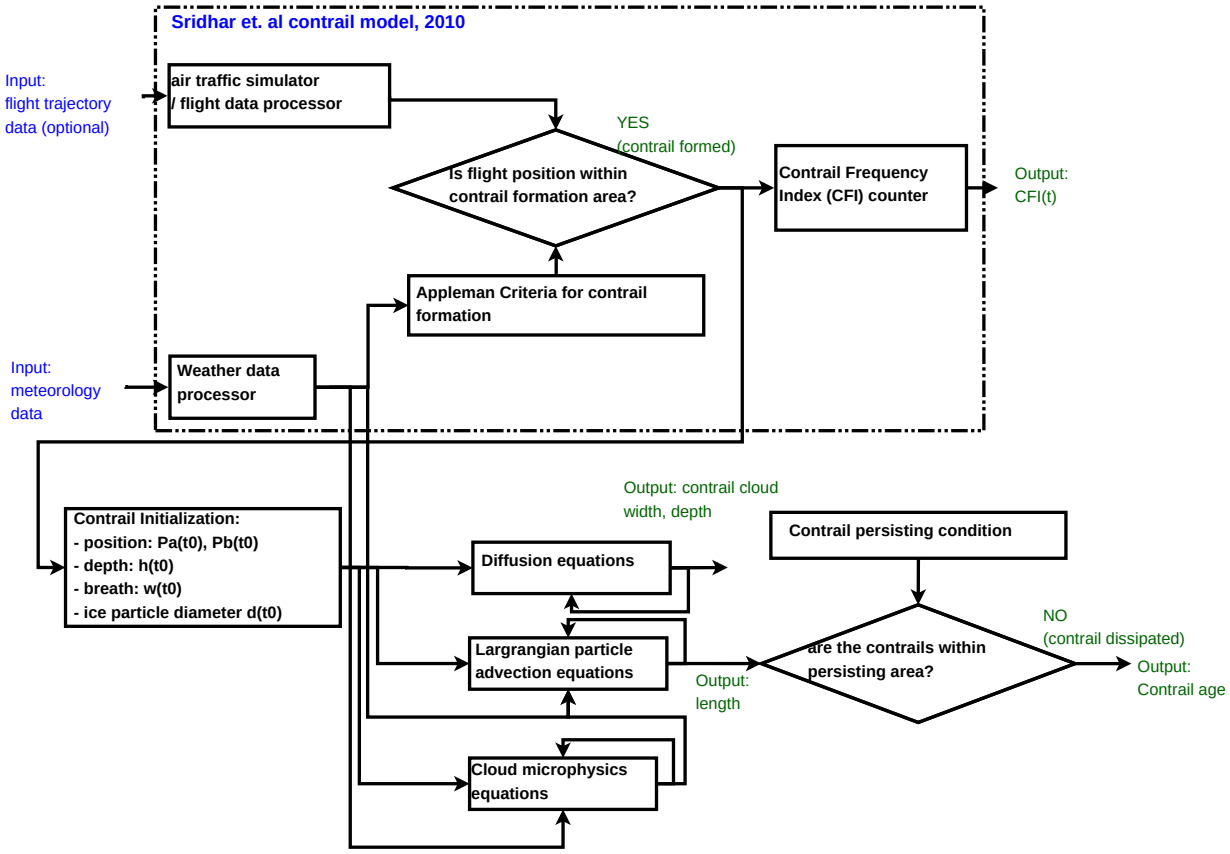

Figure 1: Dynamic contrail model structure

Rapid Update Cycle (RUC) or Rapid Refresh (RAP) models. RH_i is the relative humidity with respect to ice that can be derived from RH_w as:

$$RH_i = RH_w \frac{6.0612 \exp(18.102T/(249.15+T))}{6.1162 \exp(22.577T/(273.78+T))}. \tag{2}$$

Finally, r_{contr} and T_{contr} are the relative humidity and temperature thresholds respectively, defined as:

$$\begin{aligned} T_{contr} &= -46.46 + 9.43\ln(G-0.053) + 0.72\ln^2(G-0.053) + 273.15, \\ r_{contr} &= \frac{G(T-T_{contr})+e^{liq}_{sat}(T_{contr})}{e^{liq}_{sat}(T)}, \end{aligned} \tag{3}$$

where water vapor pressure ratio $e^{liq}_{sat}(T) = 6.0612\exp(\frac{18.102T}{249.52+T})$, $G = \frac{EI_{H_2O}C_pPr}{\epsilon Q(1-\eta)}$, water vapor emission index $EI_{H_2O} = 1.25$, air heat capacity $C_p = 1.004 \times 10^3 JKg^{-1}K^{-1}$, ambient air pressure Pr, ratio of molecular masses of water and dry air $\epsilon = 0.6222$, and average propulsion efficiency of the jet engine $\eta = 0.3$.

Once the contrails were formed, they can persist in an ice-saturated environment, i.e. those where

$$RH_i > RH_{iC} \tag{4}$$

The critical value RH_{iC} is set to be 80% in the model.

In summary, in the proposed dynamic aircraft contrail model, given a region of airspace centered at (x=latitude, y=longitude, z=altitude), if the ambient relative humidity $RH_w(x,y,z,t)$ and ambient temperature $T(x,y,z,t)$ satisfy (1), persistent contrails are formed immediately after an aircraft flies through the region within a short time interval around t. The contrails will persist as long as the ambient relative humidity with respect to ice $RH_i(x,y,z,t)$ satisfies (4).

II.B. Contrail Lagrangian dispersion model

Young-age linear contrails are modeled using a cuboid as shown in Fig. 2. It assumes that the contrails consist of spherical ice crystals only. Linear contrails can travel a long distance through airspace, driven by the ambient wind field and gravitational force. Also, the geometry of the contrail will grow by diffusion.

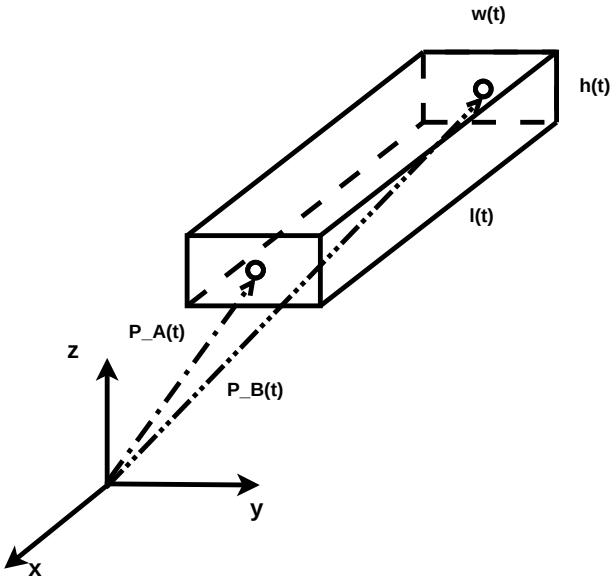

Figure 2: Geometry model of the linear contrail

Let $p(t) := [x(t)\ y(t)\ z(t)]^T$ represent the contrail end-point position at time t. The wind field near $p(t)$ is $u(p(t),t) := [x_w(p(t),t)\ y_w(p(t),t)\ z_w(p(t),t)]^T$. Here $u(t) := [x_w(t)\ y_w(t)\ z_w(t)]^T$ is used for simplicity.

The advection of linear contrails is calculated assuming Lagrangian dispersion model as follows:

$$\begin{cases} x(t+\Delta t) = x(t) + x_w(t)\Delta t, \\ y(t+\Delta t) = y(t) + y_w(t)\Delta t, \text{ and} \\ z(t+\Delta t) = z(t) + (z_w(t) + z_s(t))\Delta t, \end{cases} \tag{5}$$

where Δt is the sample time, and z_s is the ice particle settling velocity (or terminal velocity). z_s is calculated using Stokes equation for small ice particles (less than $100\mu m$):[23]

$$z_s(t) = -g\rho_i d_i^2(t)/18\eta,\ \forall d_i \leq 100 \tag{6}$$

where ρ_i is the ice density, d_i is the ice particle diameter, η is the gas viscosity coefficient, and g is the gravitational acceleration. For large ice particles (greater than $100\mu m$), an empirical equation from reference[15] is used to approximate the ice crystal terminal velocity as:

$$z_s = 9(100d_i)^{0.8},\ \forall d_i > 100 \tag{7}$$

The length of the contrail is then calculated by the distance between the end points $p_A(t)$ and $p_B(t)$ as shown in Fig. 2.

$$l(t) = |p_A(t) - p_B(t)|. \tag{8}$$

Next, the growth of contrail width and depth because of turbulent mixing is modeled using the following diffusion equations:

$$\begin{cases} h(t+\Delta t) = D_v\Delta t/h(t) + h(t), \\ w(t+\Delta t) = D_h\Delta t/w(t) + w(t) \end{cases} \tag{9}$$

where D_h and D_v are diffusion coefficients in the horizontal and vertical directions respectively, as used in the DLR and Stanford aircraft contrail model.

II.C. Cloud microphysics model

The ice particle growth due to ambient water vapor deposition on the ice crystal surface is modeled as follows:

$$d_i(t + \Delta t) = d_i(t) + r_d(\alpha)\Delta t, \tag{10}$$

where α is a deposition coefficient and $r_d(\alpha)$ represents the particle diameter rate of growth. The detailed ice crystal growth model is in the Appendix. Note that the time-varying ice particle diameter $d_i(t)$ in eq. (10) is directly related to the particle settling velocity in eq. (6) or (7) and thus control the contrail vertical movement in eq. (5).

II.D. Contrail life span

Contrails may persist if they are within a persistent contrail favorable region as defined in eq. (4). Let $\Omega(t)$ represent a set of all persistent contrail favorable regions at t. For any contrail trajectory $\{p(t),\ t \geq t_0\}$ calculated using (5), the contrail life span $t_f - t_0$ (or maximum contrail age) is defined as followed:

$$t_f = \min\{t \geq t_0 | p(t) \notin \Omega(t)\}, \tag{11}$$

where t_0 is the initial contrail formation time and $p(t_0)$ is the initial contrail formation location.

In summary, eq. (5) is applied only for the contrail life cycle $t \in [t_0, t_f]$ from (11). The contrail geographical locations and the lengths are calculated using eqs. (5)-(8) and (10). The contrail depths and widths are calculated independently using eq. (9).

III. Results

In this section, aircraft contrails are simulated using the dynamic contrail model developed in Section II. The model is used with 24-hour air traffic and meteorological data beginning at 0800UTC, April 12, 2010. The continental U.S. airspace is divided into small cuboid grid cells, where the horizontal grid size is approximately 13km $\times$ 13km (the same as the grid cells of NOAA's Rapid Update Cycle (RUC) or Rapid Refresh (RAP) data) and the vertical grid size is 1000 feet. There are a total of 451×337 grid cells required to cover the entire continental U.S. airspace horizontally and 21 vertical levels from FL240 (24,000ft) to FL440 (44,000ft) that cover the majority of persistent contrail formation areas. Sample time Δt is chosen to be one hour, in accordance with RUC update rate. The initial contrail properties (cloud width and depth, average ice particle diameter) and contrail model parameters (horizontal and vertical-direction diffusion coefficients, deposition coefficient) are set to values suggested in literature:[16,24]

$$\begin{aligned} w(t_0) &= 10m, \\ h(t_0) &= 100m, \\ d_i(t_0) &= 8\mu m, \\ D_h &= 20m^2/s, \\ D_v &= 0.6m^2/s, \text{ and} \\ \alpha &= 0.036. \end{aligned} \tag{12}$$

III.A. Contrail dispersion

The contrail width and depth in eq. (9) are functions of contrail age only. Given the initial values from (12), Fig. 3 shows the contrail width and depth diffusive growth with respect to age.

From Fig. 3, the linear contrail width disperses at a faster rate than depth growth. For example, the contrail width grows 93 times while the contrail depth grows less than 2 times in the first six hours. The results are required to compute the radiative forcing, which measures the global temperature change.

III.B. Contrail advection

The dynamic contrail model can track each contrail trajectory for its entire life cycle. It took about $3-6$ hours (including processing real-time meteorological and air traffic data) to simulate 24-hour aircraft contrails for

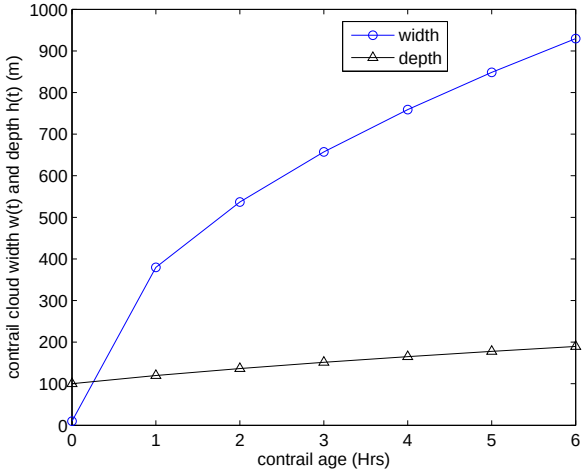

Figure 3: The diffusive growth of young-age linear contrail width $w(t)$ and depth $h(t)$

the entire continental U.S. airspace using a duo-core desktop computer. Figure 6 illustrates the first 6-hours of advection of a set of contrails originated at 0800UTC on Apr. 12, 2010, where the contrails' vertical position is represented by colors. Figure 6 shows that the contrails travel both vertically and horizontally in the ice saturated environment, depending on local wind conditions. The contrail trajectory is required to calculate the radiative forcing, assuming non-uniform and time-varying solar radiation.

III.C. Life span of potential persistent contrail formation regions

Potential persistent contrail formation regions can be computed using the Appleman criterion in eq. (1) given the meteorological data. Next, the life span of each potential persistent contrail formation grid cell can be computed using eq. (11) by tracking the contrail trajectories. Figure 4 shows a sample of potential persistent contrail formation regions over the continental U.S. airspace near 40,000 feet at 1700UTC on Apr. 12, 2010, where the life span of each grid cell is represented by colors. April 12 actually has some of the most severe potential persistent contrail coverages in 2010. Figure 4 (left) shows that a majority of mid-west U.S. airspace near $40,000$ feet between $1700-1800$UTC is covered by potential persistent contrail formation regions. Among all Air Route Traffic Control Centers (ARTCCs) that have been affected near that altitude, Denver Center (ZDV) has the largest percentage of airspace covered by potential persistent contrail formation regions that will last 6 hours or longer. This provides valuable information when planning air traffic to alleviate climate impact resulting from aircraft contrails. Next, Fig. 4 (right) highlights only the grid cells that were actually triggered by aircraft that flew on that day. It further shows that ZDV indeed experienced a significant aircraft contrail impact during that hour.

III.D. Contrail Frequency Index

The Contrail Frequency Index (CFI), which was first introduced by Chen,[8] is defined as the total number of aircraft that fly through potential persistent contrail formation grid cells. It provides a quantitative metric to measure aircraft contrail impact. In this paper, CFI is extended to account for contrail life spans using the dynamic contrail model, defined as follows:

$$CFI(I,t) = (t_f(I,t) - t) \times N(I,t), \tag{13}$$

where I is the airspace grid cell index, $(t_f - t)$ is the contrail life span, and $N(I,t)$ is the number of aircraft that fly through cell I at t. Figure 5 shows the total CFIs of 20 ARTCCs on April 12, 2010. As indicated in Fig. 4, Denver Center (ZDV) has the highest total CFI.

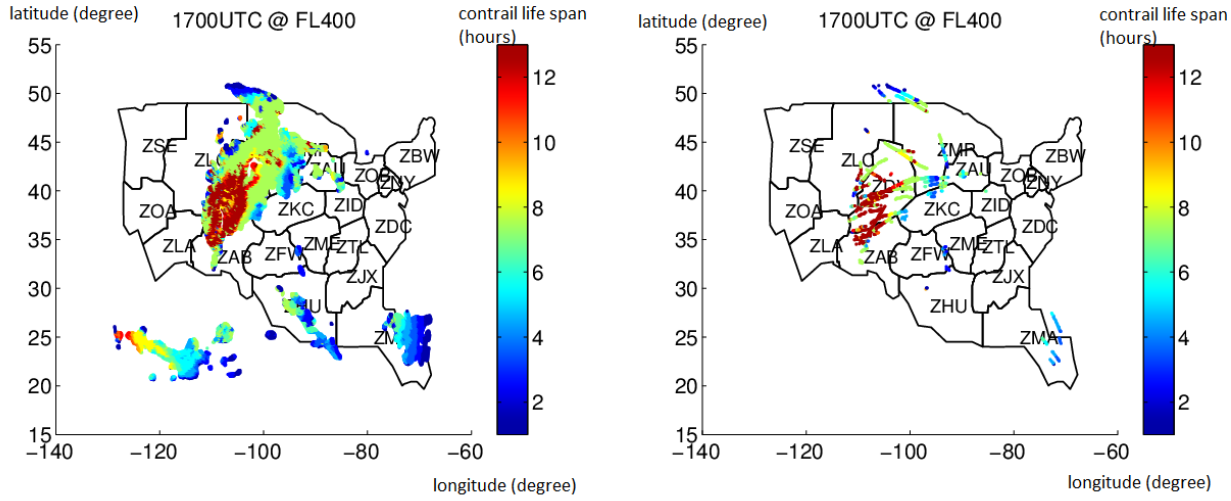

Figure 4: (left) Potential persistent contrail formation regions; and (right) contrails that were triggered by aircraft using real-time air traffic data.

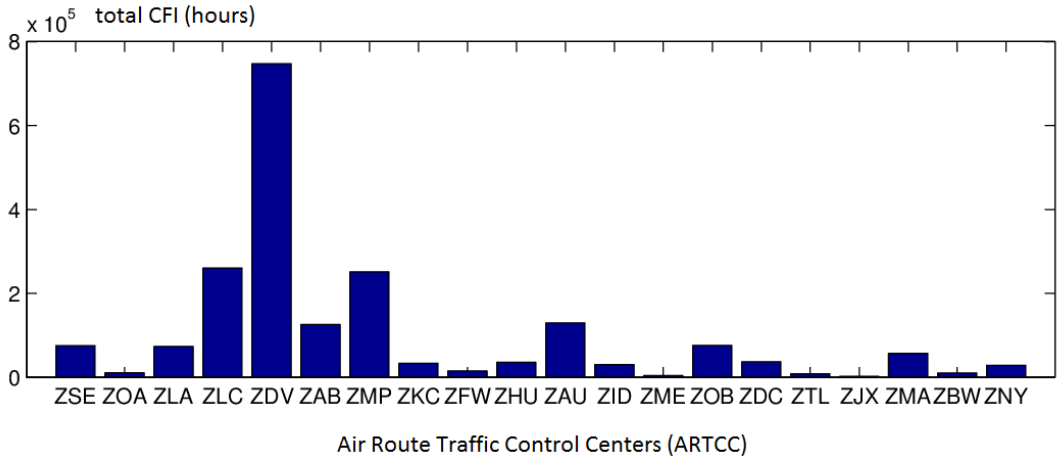

Figure 5: Accumulated 24-hour CFI distributed by center on April 12, 2010

IV. Conclusion

In this paper, the aircraft contrail model developed at NASA Ames Research Center has been extended to simulate the full life cycle of aircraft-induced young-age linear contrails by adding a Lagrangian dispersion model and a cloud microphysics model. It can simulate 24-hour aircraft contrails over the continental U.S. airspace with real-time meteorological and air traffic data in $3-6$ hours, which is computationally efficient compared with the other aircraft contrail simulation models based on our knowledge. Finally, some initial simulation results demonstrate the capabilities of the proposed model to simulate the aircraft contrail trajectories. The results, including ice particle sizes, contrail ages, and contrail cloud horizontal cover areas, are important because they are required to compute the radiative forcing, which measure the global temperature change resulting from aviation-induced contrails. Additional future work includes contrail radiative forcing computation. It is also necessary to validate the results with live contrails from satellite images and/or the results from the other aircraft contrail simulators such as DLR's CoCiP.

Appendix: Contrail ice particle growth model

For completeness, here $r_d(\alpha)$ in eq. (10) is derived in detail using the cloud microphysics model from references.[15,25]

1. Let D_v in m^2/s be the diffusivity of water vapor in air for temperature, between -40 and 40^oC.

$$D_v = 0.211 \left(\frac{T}{T_0}\right)^{1.94} \left(\frac{p_0}{p}\right) 10^{-4}, \tag{14}$$

where T and $T_0 = 273.15K$ are reference and standard temperature; and p and $p_0 = 101325Pa$ are reference and standard pressure, respectively.

Let λ in meter be the mean free path of air molecules.

$$\lambda = \frac{2\mu}{p\sqrt{\frac{8m_{air}}{\pi RT}}}, \tag{15}$$

where $\mu = 1.83 \times 10^{-5}$ is the viscosity of air; $m_{air} = 28.97 \times 10^{-3}$kg/mol is the molecular mass of air; and $R = 8.214$J/K/mol is the gas constant.

Then the modified diffusivity of water vapor for the kinetic correction is calculated as:

$$D_v^{'} = \frac{D_v}{\frac{r(t)}{r(t)+\Delta_v} + \frac{D_v}{r(t)\alpha}\sqrt{\frac{2\pi M_w}{RT}}}, \tag{16}$$

where $r(t)$ is the particle radius, α is the deposition coefficient; $\Delta_v = 1.3\lambda$ and $M_w = 0.018$kg/mol is the ratio of the molecular mass of water and dry air, $Q = 43 \times 10^6 JKg^{-1}$ is the specific combustion heat, and $\eta = 0.3$ is the average propulsion efficiency of the jet engine.

Let $\kappa_a^{'}$ be the modified thermal conductivity of water vapor for the kinetic correction.

$$\kappa_a^{'} = \frac{\kappa_a}{\frac{r(t)}{r(t)+\Delta_T} + \frac{\kappa_a}{r(t)\alpha_T \rho_{air} c_p}\sqrt{\frac{2\pi M_w}{RT}}}, \tag{17}$$

where $\kappa_a = 0.025$J/s/m/C is the thermal conductivity of water vapor; $\Delta_T = 2.16 \times 10^{-7} m$ is the thermal accommodation coefficient; $\alpha_T = 0.7$; ρ_{air} is the air density; and $c_p = 1 \times 10^3$J/kg/K is the specific heat of dry air.

Let $e_{sat,i}$ be the saturation vapor pressure with respect to ice,

$$e_{sat,i} = e^{9.55 - \frac{5723.3}{T} + 3.53\log(T) - 0.0073T}. \tag{18}$$

Let $e_{sat,w}$ in Pa be the saturation vapor pressure with respect to water,

$$e_{sat,w} = 611.2e^{\frac{17.62(T-273.15)}{243.12+(T-273.15)}}. \tag{19}$$

Let L_s be the specific latent heat of sublimation,

$$L_s = (2834.1 - 0.29T - 0.004T^2)10^3. \tag{20}$$

2. The mass growth rate of single ice particle $r_m(t)$ is calculated as:

$$r_m(\alpha) = \frac{4\pi C S_{V,i}}{\frac{\rho_i RT}{e_{sat,i} D_v^{'} M_w} + \frac{L_s \rho_i}{\kappa_a^{'} T}\left(\frac{L_s M_w}{RT} - 1\right)}, \tag{21}$$

where $C = r(t)$ is the capacitance factor of a spherical ice particle; and $S_{V,i} = \frac{e_{sat,w}}{e_{sat,i}} - 1$ is the supersaturation with respect to ice.

3. Finally, the diameter growth rate of a single ice particle $r_d(\alpha)$ in eq. (10) is calculated as:

$$r_d(\alpha) = \frac{2r_m(\alpha)}{\rho_i 4\pi r^2(t)}. \tag{22}$$

References

[1]Burkhardt, U., Krcher, B., and Schumann, U., "Global modelling of the contrail and contrail cirrus climate impact," *Bulletin of the American Meteorological Society*, Vol. 91, 2012.

[2]Burkhardt, U. and Karcher, B., "Global radiative forcing from contrail cirrus," *Nature Climate Change*, Vol. 1, 2011, pp. 54–58.

[3]FAA, "Aviation environmental and energy policy statement," Tech. rep., 2012.

[4]Lee, D., Fahey, D., Forster, P., Newton, P., Wit, R., Lim, L., Owen, B., and Sausen, R., "Aviation and global climate change in the 21st century," *Atmospheric Environment*, Vol. 43, 2009, pp. 3520–3537.

[5]Burkhardt, U. and Krcher, B., "Process-based simulation of contrail cirrus in a global climate model," *Journal of Geophysical Research*, Vol. 114, 2009.

[6]Naiman, A. D., Lele, S. K., Wilkerson, J. T., and Jacobson, M. Z., "A low order contrail model for use with global-scale climate models," *47th AIAA Aerospace Science Meeting*, Orlando, FL, 2009.

[7]Sridhar, B., Ng, H. K., and Chen, N. Y., "Aircraft Trajectory Optimization and Contrails Avoidance in the Presence of Winds," *10th AIAA Aviation Technology, Integration and Operations Conference (ATIO)*, Fort Worth, TX, 2010.

[8]Chen, N. Y., Sridhar, B., and Ng, H. K., "Prediction and use of contrail frequency index for contrail reduction strategies," *AIAA Guidance, Navigation, and Control Conference*, Toronto, Canada, 2010.

[9]Naiman, A. D., Lele, S. K., and Jacobson, M. Z., "Large Eddy simulations of persistent aircraft contrails," *49th AIAA Aerospace Science Meeting*, Orlando, FL, 2011.

[10]Jacobson, M. Z., Wilkerson, J. T., Naiman, A. D., and Lele, S. K., "The effects of aircraft on climate and pollution. Part I: Numerical methods for treating the subgrid evolution of discrete size- and composition-resolved contrails from all commercial flights worldwide," *Journal of Computational Physics*, Vol. 230, 2011, pp. 5115–5132.

[11]Schumann, U., "A contrail cirrus prediction model," *Geoscientific Model Development*, Vol. 5, 2012, pp. 543–580.

[12]DeGrand, J., Carleton, A. M., Travis, D. J., and Lamb, P. J., "A satellite-based climatic description of jet aircraft contrails and associations with atmospheric conditions: 1977-79," *Journal of Applied Meteorology*, Vol. 39, 2000, pp. 1434–1459.

[13]Minnis, P., Palikonda, R., Walter, B., Ayers, J., and Mannstein, H., "Contrail properties over the eastern North Pacific from AVHRR data," *Meteorol. Z.*, Vol. 14, 2005, pp. 515–523.

[14]Duda, D. P., Minnis, P., and Nguyen, L., "Estimates of cloud radiative forcing in contrail clusters using GOES imagery," *Journal of Geophysical Research: Atmospheres*, Vol. 106, 2001, pp. 4927–4937.

[15]Pruppacher, H. R. and Klett, J. D., *Microphysics of clouds and precipitation*, Kluwer Academic, Norwell, Mass, 2000.

[16]Schumann, U., P, P. K., Baumann, R., Busen, R., Gerz, T., Schlager, T., Schulte, P., and H, H. V., "Estimate of diffusion parameters of aircraft exhaust plumes near the tropopause from nitric oxide and turbulence measurements," *Journal of Geophysical Research*, Vol. 100, 1995, pp. 147–162.

[17]Burkhardt, U., Karcher, B., and Schumann, U., "Global modeling of the contrail and contrail cirrus climate impact," *Bulletin of the American Meteorological Society*, Vol. 91, No. 5, 2010, pp. 479–483.

[18]Chen, N. Y., Sridhar, B., and Ng, H. K., "Tradeoff between Contrail Reduction and Emissions in United States National Airspace," *Journal of Aircraft*, Vol. 49, No. 5, 2012, pp. 4–23.

[19]Sridhar, B., Chen, N. Y., and Ng, H. K., "Energy Efficient Contrail Mitigation Strategies for Reducing the Environmental Impact of Aviation," *10th USA/Europe Air Traffic Management Reserach and Development Seminar*, Chicago, IL, 2013.

[20]Appleman, H., "The formation of exhaust contrails by jet aircraft," *Bulletin of the American Meteorological Society*, Vol. 34, 1953, pp. 14–20.

[21]Schumann, U., "On conditions for contrail formation from aircraft exhausts," *Meteorol. Zeitschrift*, Vol. 5, 1996, pp. 4–23.

[22]Sridhar, B., Chen, N. Y., and Ng, H. K., "Design of aircraft trajectories based on trade-offs between emission sources," *9th USA/Europe Air Traffic Management Research and Development Seminar*, 2011.

[23]Seinfeld, J. H. and Pandis, S. N., *Atmospheric chemistry and physics: from air pollution to climate change*, John Wiley and Sons, 2nd ed., 2006.

[24]Chlond, A., "Large-Eddy Simulation of Contrails," *Journal of Atmospheric Sciences*, Vol. 5, 1997, pp. 796–819.

[25]Gierens, K. M., M, M. M., and Gayet, J. F., "The deposition coefficient and its role for cirrus clouds," *Journal of Geophysical Research*, Vol. 108, 2003.

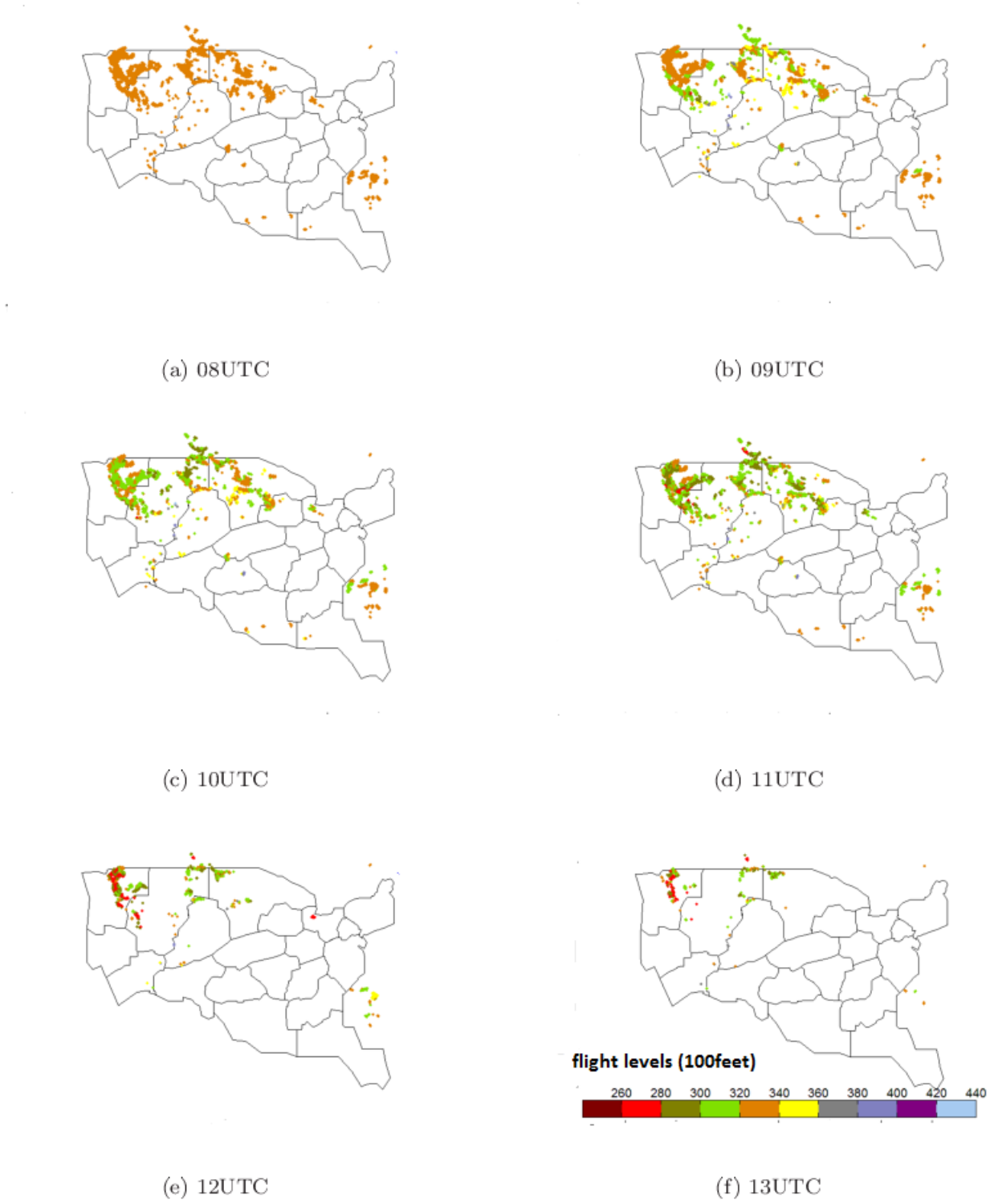

(a) 08UTC (b) 09UTC

(c) 10UTC (d) 11UTC

(e) 12UTC (f) 13UTC

Figure 6: Advection for contrails that were originated at 0800UTC on Apr. 12, 2010